

Accepted Manuscript

Highly-efficient *N*-arylation of imidazole catalyzed by Cu(II) complexes with quaternary ammonium-functionalized 2-acetylpyridine acylhydrazone

Milica R. Milenković, Argyro T. Papastavrou, Dušanka Radanović, Andrej Pevec, Zvonko Jagličić, Matija Zlatar, Maja Gruden, Georgios C. Vougioukalakis, Iztok Turel, Katarina Anđelković, Božidar Čobeljić

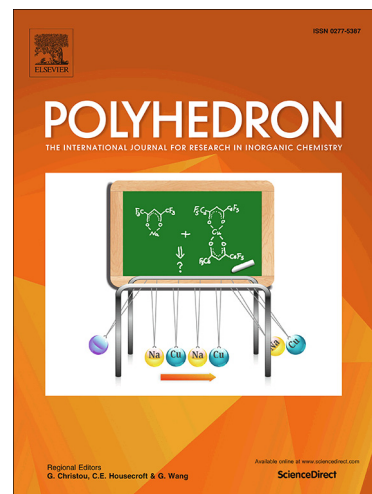
PII: S0277-5387(19)30166-4
DOI: <https://doi.org/10.1016/j.poly.2019.03.001>
Reference: POLY 13801

To appear in: *Polyhedron*

Received Date: 25 January 2019
Revised Date: 28 February 2019
Accepted Date: 2 March 2019

Please cite this article as: M.R. Milenković, A.T. Papastavrou, D. Radanović, A. Pevec, Z. Jagličić, M. Zlatar, M. Gruden, G.C. Vougioukalakis, I. Turel, K. Anđelković, B. Čobeljić, Highly-efficient *N*-arylation of imidazole catalyzed by Cu(II) complexes with quaternary ammonium-functionalized 2-acetylpyridine acylhydrazone, *Polyhedron* (2019), doi: <https://doi.org/10.1016/j.poly.2019.03.001>

This is a PDF file of an unedited manuscript that has been accepted for publication. As a service to our customers we are providing this early version of the manuscript. The manuscript will undergo copyediting, typesetting, and review of the resulting proof before it is published in its final form. Please note that during the production process errors may be discovered which could affect the content, and all legal disclaimers that apply to the journal pertain.



Highly-efficient *N*-arylation of imidazole catalyzed by Cu(II) complexes with quaternary ammonium-functionalized 2-acetylpyridine acylhydrazone

Milica R. Milenković^a, Argyro T. Papastavrou^b, Dušanka Radanović^c, Andrej Pevec^d, Zvonko Jagličić^e, Matija Zlatar^c, Maja Gruden^a, Georgios C. Vougioukalakis^b, Iztok Turel^d, Katarina Anđelković^{a,*} and Božidar Čobeljić^{a,*}

^aUniversity of Belgrade, Faculty of Chemistry, Studentski trg 12-16, 11000 Belgrade, Serbia

^bLaboratory of Organic Chemistry, Department of Chemistry, National and Kapodistrian University of Athens, Panepistimiopolis, 15771 Athens, Greece

^cInstitute of Chemistry, Technology and Metallurgy, University of Belgrade, Njegoševa 12, P.O. Box 815, 11000 Belgrade, Serbia

^dFaculty of Chemistry and Chemical Technology, University of Ljubljana, Večna pot 113, 1000 Ljubljana, Slovenia

^eInstitute of Mathematics, Physics and Mechanics & Faculty of Civil and Geodetic Engineering, University of Ljubljana, Jadranska 19, Ljubljana, Slovenia

Abstract

The reaction of (*E*)-*N,N,N*-trimethyl-2-oxo-2-(2-(1-(pyridin-2-yl)ethylidene)hydrazinyl)ethan-1-aminium-chloride (**HLCI**) with copper(II) perchlorate led to mononuclear [CuLCl]ClO₄ complex (**1**). The same reaction with excess of sodium azide gives dinuclear azido double end-on bridged Cu(II) complex [Cu₂L₂(μ-1,1-N₃)₂](ClO₄)₂ (**2**). In both complexes hydrazone ligand is NNO

*Corresponding Authors:

Katarina Anđelković

E-mail: kka@chem.bg.ac.rs

ORCID: 0000-0003-1178-8326

Božidar Čobeljić

E-mail: bozidar@chem.bg.ac.rs

ORCID: 0000-0001-6335-0196

coordinated in monodeprotonated formally neutral zwitter-ionic form. Complexes were characterized by elemental analysis, IR spectroscopy and single- crystal X- ray crystallography. Variable- temperature magnetic susceptibility measurements for dinuclear Cu(II) complex showed intra-dimer ferromagnetic coupling between Cu(II) ions ($J = 7.4 \text{ cm}^{-1}$). DFT-BS calculations provided explanation for magnetic properties of dinuclear Cu(II) complex. Both complexes were shown to highly efficiently catalyze the *N*-arylation of imidazole and benzimidazole with electron-poor or electron-rich aryl iodides, under user-friendly and sustainable conditions.

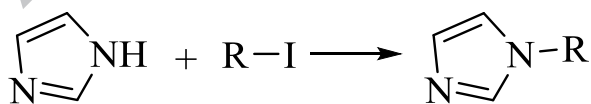
Keywords: Cu(II) complexes, hydrazones, DFT calculations, crystal structure, catalysis

1. Introduction

Polynuclear transition metal complexes with bridging ligands are a promising class of compounds for the development of magnetic materials and understanding magneto-structural correlations [1–6]. Pseudohalides (azide, cyanate, thiocyanate, etc.) have widely been used for the synthesis of such systems, because of their ability to coordinate metal ions in different modes, as monodentate or bridging ligands. The bridging modes strongly influence the magnetic interactions between adjacent metal ions, ranging from antiferromagnetic to ferromagnetic couplings of spins on paramagnetic centers. In general, the type and magnitude of the magnetic interactions depend on the $M \cdots M$ separation, $M-X$ bond length, $M-X-M$ and $X-M-X$ angles, the dihedral angles between the planes containing the metal ions and the symmetry of the bridging mode [7]. A homonuclear azido ligand can bind transition metal ions as monodentate or bridging ligand, leading to the formation of mononuclear or polynuclear species, respectively. As bridging bidentate ligand, the azide anion binds the metals via EO (end-on) or EE (end-to-end) mode forming the following bridges: $\mu_{1,1}-N_3$ (single EO), $di-\mu_{1,1}-N_3$ (double EO), $\mu_{1,3}-N_3$ (single EE) and $di-\mu_{1,3}-N_3$ (double end-to-end). The other coordination modes, including tridentate bridges $\mu_{1,1,1}-N_3$ and $\mu_{1,1,3}-N_3$ and rarer, tetradentate ones $\mu_{1,1,1,1}-N_3$, $\mu_{1,1,3,3}-N_3$ and $\mu_{1,1,1,3,3,3}-N_3$, afford complexes with variable nuclearity, magnitude and type of exchange coupling (antiferromagnetic or ferromagnetic) between the paramagnetic metalcenters [3].

From a synthetic point of view, it is not an easy task to predict the structure of metallo-pseudohalide complexes obtained in the reaction of a transition metal salt, a pseudohalide ligand and a blocking polydentate ligand. In the case of a particular pseudohalide, the nuclearity of reaction product depends on metal ion, counter anion, organic (blocking) ligand, stoichiometric ratio of the reactants, solvent, etc. Several NNO donor Schiff bases are used as blocking ligands in polynuclearazide bridged complexes [4,8–11]. Acylhydrazone ligands are of particular interest, since they exhibit keto-enol tautomerism and can coordinate metal ions in neutral or deprotonated forms, increasing the diversity of their coordination compounds [7,8,10–14]. Girard's reagents [Girard's T (trimethylacetylhydrazide ammonium chloride), Girard's D (*N,N*-dimethylglycine hydrazide hydrochloride), and Girard's P (pyridinioacetohydrazide chloride)] are *N*-substituted glycine hydrazides [15], which readily reacts with carbonyl group forming water soluble hydrazones. Girard's T reagent hydrazones are quaternary ammonium salts, which can coordinate metal ions either in their non-deprotonated, positively charged form, or in their deprotonated, formally neutral, zwitter-ionic form. In recent years, one part of our research is oriented towards the investigation of the structural and magnetic properties of pseudohalide metal complexes with hydrazones of Girard's T reagent [15].

On a different note, the synthesis of imidazole-based compounds is very important due to their numerous applications, amongst others as drugs, agrochemicals, and biomimetic catalysts [16–20]. The *N*-arylimidazole scaffold, for example, is a moiety found in many biologically-active natural products and pharmaceutically-related compounds with applications for diseases such as congestive heart failure and myocardial fibrosis. These structures can be easily prepared through *N*-substitution of imidazole [21,22]. One of the most promising strategy in forming the corresponding C-N bond is the copper-catalyzed *N*-arylation of imidazoles with aryl halides, (**Scheme 1**) [23] a transformation studied for the first time by Ullmann [24–30]. In this regard, a number of Cu-based catalytic systems, employing salen or chelating Schiff base ligands, have been found to catalyze these types of reactions in the past [31–35].



Scheme 1. Copper-catalyzed *N*-arylation of imidazoles with aryl halides.

Herein, we report on the synthesis, structural and magnetic characterization of mono (**1**) and dinuclear (**2**) Cu(II) complexes with the condensation product of 2-acetylpyridine and Girard's T reagent. The experimental studies on the magnetic properties of dinuclear azide bridged Cu(II) complex have been accompanied by the density functional theory (DFT) calculations. Also, we explored the catalytic activity of the complexes **1** and **2** in the *N*-arylation of imidazole and benzimidazole under sustainable, user-friendly and low-cost conditions.

2. Experimental

2.1. Materials and methods

2-Acetylpyridine ($\geq 99\%$) and Girard's T reagent (99%) were obtained from Aldrich. IR spectra were recorded on a Nicolet 6700 FT-IR spectrometer using the ATR technique in the region 4000–400 cm^{-1} (s-strong, m-medium, w-weak). Elemental analyses (C, H, and N) were performed by standard micro-methods using the ELEMENTARVario ELIII C.H.N.S.O analyzer. Magnetic properties of a polygra in sample were investigated using a Quantum Design MPMS-XL-5 SQUID magnetometer. Susceptibility has been measured between 2 K and 300 K in a constant magnetic field of 1 kOe. NMR spectra were recorded with a Varian Mercury 200MHz spectrometer. GC-MS spectra were recorded with a Shimandzu R GCMS-QP2010 Plus Chromatograph Mass Spectrometer using a MEGAR (MEGA-5, F.T: 0.25 μm , I.D.: 0.25mm, L: 30m, T_{max} : 350 $^{\circ}\text{C}$, Column ID# 11475) column.

2.1.1. Synthesis of ligand **HLCl** (*E*)-*N,N,N*-trimethyl-2-oxo-2-(2-(1-(pyridin-2-yl)ethylidene)hydrazinyl)ethan-1-aminium-chloride

The ligand **HLCl** was synthesized by the reaction of Girard's T reagent (1.6764 g, 1.00 mmol) and 2-acetylpyridine (1.120 mL, 1.00 mmol) in methanol (50 mL). The reaction mixture was acidified with 3–4 drops of 2M HCl and was refluxed for 2 h at 85 $^{\circ}\text{C}$. IR: 3387 (w), 3127 (m), 3090 (m), 3049 (m), 3016 (m), 2950 (s), 1700 (vs), 1612 (w), 1549 (s), 1485 (m), 1400 (m), 1300 (w), 1253 (w), 1200 (s), 1153 (w), 1135 (m), 1095 (w), 1073 (m), 975 (w), 944 (w), 914

(m), 748 (w), 683 (w). Elemental analysis calcd for $C_{12}H_{19}ClN_4O$: C 53.23 %, H 7.07 %, N 20.69 %, found: C 53.42 %, H 7.12 %, N 20.77 %.

2.1.2. Synthesis of mononuclear Cu(II) complex (1)

The mononuclear Cu(II) complex was synthesized by the reaction of $Cu(ClO_4)_2 \cdot 6H_2O$ (111mg, 0.30 mmol) and ligand **HLCl** (70mg, 0.30 mmol) in methanol (20 mL). The solution was refluxed for 4 h. After refrigeration of the reaction solution at $-8^\circ C$ for two weeks, green crystals suitable for X-ray analysis were formed. Yield: 102mg (79 %). IR (cm^{-1}): 3096 (w), 3037 (w), 2958 (w), 1636 (w), 1603 (w), 1573 (w), 1525 (s), 1472 (m), 1447 (s), 1362 (w), 1399 (m), 1374 (w), 1339 (m), 1316 (w), 1263 (w), 1242 (w), 1152 (w), 1075 (vs), 966 (w), 930 (w), 912 (m), 815 (w), 785 (m), 754 (w), 682 (w), 647 (w), 622 (m), 568 (w). Elemental analysis calcd for $C_{12}H_{18}Cl_2CuN_4O_5$: C 33.31 %, H 4.19 %, N 12.95 %, found: C 33.27 %, H 4.22 %, N 12.78 %.

2.1.3. Synthesis of dinuclear Cu(II) complex (2)

Into a mixture of $Cu(ClO_4)_2 \cdot 6H_2O$ (111 mg, 0.30 mmol, dissolved in 5 mL of H_2O) and ligand **HLCl** (70 mg, 0.30 mmol, dissolved in 20 mL of methanol) excess of NaN_3 (52 mg, 0.90 mmol, dissolved in 5 mL of H_2O) was added. The reaction mixture was refluxed for 4 h. After refrigeration of the reaction solution at $-8^\circ C$ for two weeks, dark green crystals suitable for X-ray analysis were formed. Yield: 221mg (84 %). IR (cm^{-1}): 3518 (m), 3348 (m), 2039 (vs/bs), 1628 (w), 1597 (w), 1568 (w), 1523 (m), 1468 (w), 1372 (w), 1340 (m), 1297 (m), 1146 (w), 1078 (w), 1027 (w), 974 (w), 910 (w), 779 (w), 684 (w). Elemental analysis calcd for $C_{24}H_{36}Cl_2Cu_2N_{14}O_{10}$: C 32.81 %, H 4.13 %, N 22.32 %, found: C 32.67 %, H 4.18 %, N 22.48 %.

2.2. X-ray structure determinations

The molecular structures of complexes **1** and **2** were determined by single-crystal X-ray diffraction. Crystallographic data and refinement details are given in **Table 1**. The X-ray intensity data for **1** were collected at room temperature on a Nonius Kappa CCD diffractometer

equipped with graphite-monochromator utilizing MoK α radiation ($\lambda = 0.71073 \text{ \AA}$). Data reduction and cell refinement was carried out using DENZO and SCALPACK [36]. Diffraction data for **2** were collected at room temperature with an Agilent SuperNova dual source diffractometer using an Atlas detector and equipped with mirror-monochromated MoK α radiation ($\lambda = 0.71073 \text{ \AA}$). The data were processed by using CrysAlis PRO [37]. All the structures were solved using SIR-92 [38] (**2**) and refined against F^2 on all data by full-matrix least-squares with SHELXL-2016 [39]. All non-hydrogen atoms were refined anisotropically. All other hydrogen atoms were included in the model at geometrically calculated positions and refined using a riding model. Crystallographic data for the structures reported in this paper have been deposited with the CCDC 1886534 (for **1**) and 1886535 (for **2**).

Table 1
Crystal data and structure refinement details for **1** and **2**.

	1	2
formula	C ₁₂ H ₁₈ Cl ₂ CuN ₄ O ₅	C ₂₄ H ₃₆ Cl ₂ Cu ₂ N ₁₄ O ₁₀
Fw (g mol ⁻¹)	432.74	878.65
crystal size (mm)	0.15×0.05×0.05	0.40×0.30×0.20
crystal color	green	green
crystal system	monoclinic	monoclinic
space group	<i>P</i> 2 ₁ / <i>c</i>	<i>C</i> 2/ <i>c</i>
<i>a</i> (Å)	9.9406(2)	16.4095(6)
<i>b</i> (Å)	9.5650(2)	13.6320(6)
<i>c</i> (Å)	18.8796(5)	17.1507(8)
β (°)	94.7120(10)	108.145(5)
<i>V</i> (Å ³)	1789.04(7)	3645.7(3)
<i>Z</i>	4	4
calcd density (g cm ⁻³)	1.607	1.601
<i>F</i> (000)	884	1800

no. of collected reflns	7769	18585
no. of independent reflns	4065	5002
R_{int}	0.0202	0.0282
no. of reflns observed	3215	3826
no. parameters	249	239
$R[I > 2\sigma(I)]^a$	0.0432	0.0345
$wR_2(\text{all data})^b$	0.1328	0.0891
$Goof, S^c$	1.097	1.059
maximum/minimum residual electron density (e \AA^{-3})	+0.54/-0.67	+0.30/-0.33

$^a R = \sum |F_o| - |F_c| / \sum |F_o|$. $^b wR_2 = \{ \sum [w(F_o^2 - F_c^2)^2] / \sum [w(F_o^2)^2] \}^{1/2}$.
 $^c S = \{ \sum [(F_o^2 - F_c^2)^2] / (n/p) \}^{1/2}$ where n is the number of reflections and p is the total number of parameters refined.

2.3. Computational details

The exchange coupling constant J of a dimer **2** was calculated within broken symmetry DFT formalism [40–44] according to the Yamaguchi approach [45], from relativistic single-point calculations on the experimentally determined X-ray structure:

$$J = \frac{(E_{BS} - E_{HS})}{\langle S_{HS}^2 \rangle - \langle S_{BS}^2 \rangle}$$

E_{HS} and E_{BS} are the energies of high-spin (triplet) and broken-symmetry states, respectively. $\langle S_{HS}^2 \rangle$ and $\langle S_{BS}^2 \rangle$ are their corresponding expectation values of the spin operator. All calculations were performed with the ORCA program package (version 4.0.1.2) [46] using increased integration grids (Grid4). Scalar relativistic effects were considered at the Zero-Order-Regular-Approximation (ZORA) level [47]. BP86 functional [48–50] and ZORA-def2-TZVP [51,52] basis set for all atoms have been used. The resolution of the identity (RI) approximation [53] in the Split-RI-J variant with the scalar relativistically recontracted SARC/J [52,54,55] Coulomb fitting sets has been used. Results are rationalized based on the Mulliken atomic spin populations

and spin-density map of the high-spin state. The analysis of the overlap of the non-orthogonal corresponding orbitals [56] of the broken-symmetry solution is used as well.

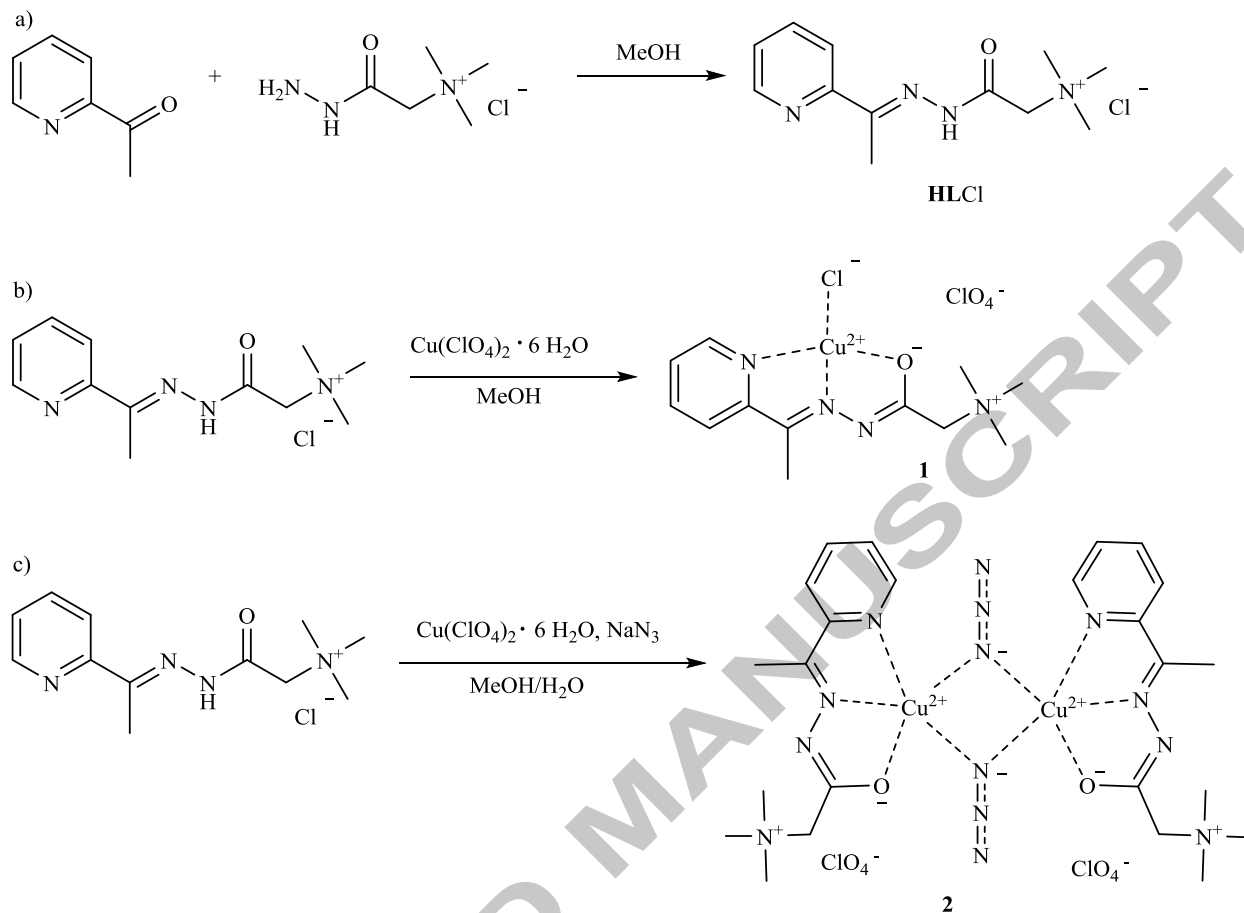
2.4. Catalysis

General procedure for the catalytic reactions: In a flame-dried vessel, equipped with a magnetic stirrer, under argon atmosphere, were added 0.3 mL of anhydrous acetonitrile, the nucleophile (imidazole or benzimidazole – 0.75 mmol, 1.5 eq.), the electrophile (alkyl or aryl iodide – 0.5 mmol, 1 eq.), the base (1 mmol, 2 eq.), and the copper catalyst (0.05 mmol – 10% loading). The reaction vessel was heated to 80 °C and left under stirring for 24 hours. The reaction mixture was then allowed to cool to room temperature, diluted with dichloromethane (5 mL) and filtered through celite. The celitepad was further washed with dichloromethane (2 × 5 mL). The combined organic phases were washed with water (2 × 5 mL) and brine (2 × 5 mL). The organic solvents were then removed in vacuo to yield the crude product, which was purified by flash column chromatography on silica gel using a gradient mixture of ethyl acetate / petroleum ether as eluent. The ¹H and ¹³C NMR spectral data for all *N*-arylatedimidazoles and benzimidazoles are in full agreement with those reported to literature [57–61].

3. Results and discussion

3.1. Synthesis

The ligand (**HLCl**), (*E*)-*N,N,N*-trimethyl-2-oxo-2-(2-(1-(pyridin-2-yl)ethylidene)hydrazinyl)ethan-1-aminium-chloride, was obtained from the condensation reaction of 2-acetylpyridine and Girard's T reagent (Scheme 2a). By the reaction of ligand **HLCl** with Cu(ClO₄)₂·6H₂O in a 1 : 1 molar ratio in methanol, mononuclear Cu(II) complex **1**, with the composition [Cu**LCl**]ClO₄, was obtained (Scheme 2b). Reaction of **HLCl** with Cu(ClO₄)₂·6H₂O and NaN₃ in a 1 : 1 : 3 molar ratios, in a mixture of methanol/water (2 : 1), gives dinuclear double end-on azido bridged Cu(II) complex **2**, with composition [Cu₂**L**₂(μ_{-1,1}-N₃)₂](ClO₄)₂ (Scheme 2c).



Scheme 2. Synthesis of ligand **HLCI** (a) and complexes **1** (b) and **2** (c).

3.2. IR Spectroscopy

IR spectra of complexes **1** and **2** show that the hydrazone ligand is coordinated in its deprotonated form. The vibration of deprotonated hydrazone moiety $\nu(\text{O}^-\text{C}=\text{N})$ appears at 1636 cm^{-1} in the spectrum of **1** and at 1628 cm^{-1} in the spectrum of **2**, compared with the band of the carbonyl group in the free ligand at 1700 cm^{-1} . Coordination of the azomethine nitrogen results in a shift of $\nu(\text{C}=\text{N})$ group, from 1612 cm^{-1} in the spectrum of **HLCI** to 1603 cm^{-1} in the spectrum of complex **1** and 1597 cm^{-1} in the spectrum of complex **2**. In the IR spectra of complexes **1** and **2**, vibrations of perchlorate anions are observed at 1075 cm^{-1} and 1078 cm^{-1} , respectively. The strong band at 2039 cm^{-1} in the spectrum of complex **2** corresponds to end-on bonded azido ligands [62].

3.3. Crystal structures of complexes **1** and **2**

Complex **1** crystallizes in the monoclinic centrosymmetric space group $P2_1/c$, with the asymmetric unit (asu) comprising one complex cation $[\text{CuLCl}]^+$ and ClO_4^- anion. The molecular structure of the complex cation $[\text{CuLCl}]^+$ with atom numbering scheme is presented in **Fig. 1**. Selected bond lengths and bond angles are listed in **Table 2**. The complex cation features a four coordinate Cu(II) center with the NNO donor set of tridentate zwitterionic ligand **L** and the Cl^- ion supplementing the fourth coordination site. The coordination geometry around Cu(II) may be described as a distorted square planar with τ_4 parameter [63] of 0.15 ($\tau_4 = \frac{360^\circ - (\alpha + \beta)}{141^\circ} \tau$, where α and β are the two largest angles around the central atom). The values of τ_4 can range from 1.00 for a perfect tetrahedral geometry to zero for a perfect square-planar geometry. Intermediate structures, including trigonal pyramidal and seesaw, fall within the range of 0 to 1.00. The *cis* bond angles (N1-Cu1-Cl1, 99.81(8)°; N2-Cu1-N1, 80.66(10)°; N2-Cu1-O1, 79.61(9)° and O1-Cu1-Cl1, 99.94(6)°) show average deviation of nearly 10° from ideal (90°). The *trans* bond angle O1-Cu1-N1 is bent and the N2-Cu1-Cl1 is almost linear (O1-Cu1-N1, 160.25(10)° and N2-Cu1-Cl1, 178.19(8)°). The tridentate NNO coordination of **L** to Cu(II) ion generates two five-membered chelation rings (Cu-N-C-C-N and Cu-N-N-C-O) fused along Cu1-N2 bond. The chelate rings are nearly coplanar, as indicated by the dihedral angle of 2.0°. The $\text{N}(\text{CH}_3)_3$ group from the side chain can occupy different positions to the rest of molecule by rotating around the C8-C9 and C9-N4 bonds. The orientation of $\text{N}(\text{CH}_3)_3$ can be described by the dihedral angle N4-C9-C8-N3 which amounts -137.7(3)°. The distance of N4 atom from the mean coordination plane (Cu1, N1, N2, O1, Cl1) is 0.731(3) Å. The present orientation of the $\text{N}(\text{CH}_3)_3$ group is supported by the intramolecular C11-H11A...O1 hydrogen bond (**Table S1** in the Supplementary material).

In the environment of the Cu(II) ion two long contacts: Cu1...O5A (2.73(1) Å) and Cu1...Cl1ⁱ (i stands for -x, -y, 1-z) (3.0003(9) Å), have been noticed. If these long Cu...O_{perchlorate} and Cu...Cl contacts are viewed as bonds, the geometry around Cu(II) ion can be described as tetragonally elongated octahedral with Cl-Cu-O_{perchlorate} bond angle of 165.0(3)°. The Cu1 and Cu1ⁱ (i = -x, -y,

1-z) ions are bridged by C11 and C11ⁱ forming the centrosymmetric dimeric unit [Cu₂L₂Cl₂](ClO₄)₂ (**Fig. 2**) with Cu...Cu separation of 3.5800(5) Å. The dimeric units are reinforced by intermolecular C-H...O hydrogen bonds involving (C11) methyl group and pyridine carbon (C2) as H-bond donors and O2 from perchlorate anion as a double acceptor (**Table S1** and **Fig. S1a** in the Supplementary material). The perchlorate anions mediate in joining the dimeric units of pseudo-octahedral geometry in two-dimensional layers parallel with (100) lattice plane by means of intermolecular C-H...O hydrogen bonds (**Table S1** and **Fig. S1a**). The adjacent layers are packed *via* C_{Me}-H...Cl and C_{Me}-H...O_{perchlorate} intermolecular hydrogen bonds to form three-dimensional supramolecular structure (**Table S1** and **Fig. S1b** in the Supplementary material).

Table 2Selected bond lengths (Å) and angles (°) for **1** and **2**.

1		2	
Cu1-N1	2.011(2)	Cu1-N1	2.0272(16)
Cu1-N2	1.926(2)	Cu1-N2	1.9266(17)
Cu1-O1	1.983(2)	Cu1-O1	1.9800(14)
Cu1-Cl1	2.2157(8)	Cu1-N5	1.9333(17)
O1-C8	1.286(4)	O1-C8	1.277(2)
N3-C8	1.310(4)	N3-C8	1.317(2)
N2-C6	1.281(4)	N2-C6	1.284(2)
N2-N3	1.384(3)	N2-N3	1.381(2)
		N5-N6	1.189(2)
		N6-N7	1.140(3)
N2-Cu1-O1	79.61(9)	N2-Cu1-N5	175.54(7)
N2-Cu1-N1	80.66(10)	N2-Cu1-O1	79.91(6)
O1-Cu1-N1	160.25(10)	N5-Cu1-O1	101.92(6)
N2-Cu1-Cl1	178.19(8)	N2-Cu1-N1	79.85(7)
O1-Cu1-Cl1	99.94(6)	N5-Cu1-N1	98.57(7)
N1-Cu1-Cl1	99.81(8)	O1-Cu1-N1	159.34(7)
		N7-N6-N5	175.8(3)

Complex **2** crystallizes in the monoclinic space group $C2/c$, with the asymmetric unit (asu) containing one Cu(II) center, zwitterionic ligand **L**, one azide N_3^- ligand and ClO_4^- anion. The crystal structure displays a centrosymmetric dinuclear complex with the crystallographically independent Cu(II) center coordinating to the three donor atoms (N1, N2 and O1) from the deprotonated ligand **L** and two N atoms belonging to two bridging azido ligands (**Fig. 3**). The coordination geometry of the crystallographically independent Cu1 center is distorted square pyramidal, with the base formed by pyridyl (N1) and imine (N2) nitrogen atoms, an enolate oxygen (O1) of **L** and one azide nitrogen atom (N5), while the axial position is occupied by a nitrogen atom of another azide ($N5^{ii}$, $ii = 1.5-x, 1/2-y, 1-z$). The coordination polyhedron around Cu(II) may be described as an axially elongated square pyramid with an index of trigonality (τ_5) [64] of 0.27 [$\tau_5 = (\beta - \alpha)/60$, where β and α are the two largest angles around the central atom; τ_5 is 0 for regular square based pyramidal geometry and 1 for regular trigonal bipyramidal geometry]. For more information about the bond distances and angles see **Table 2**. The structural parameters correlating the geometry of related square pyramidal di($\mu_{-1,1}$ -azido) bridged Cu(II) complexes with hydrazone-based ligands [7,10,12–14 and this work] are listed in **Table 3**. The τ_5 value calculated for the complex **2** lies within a range of values 0.22–0.29 obtained for complexes **3–7** (**Table 3**). The azide anion bridges in an asymmetric (basal–apical) fashion so that the Cu– N_{azide} bond lengths are significantly different, Cu1–N5 1.9333(17) Å and Cu1– $N5^{ii}$ is 2.590(2) Å. The basal–apical Cu– N_{azide} bond lengths observed in **2** are comparable to those observed in complexes **3–7** [7,10,12–14]. The di- $\mu_{1,1}$ -azide bridging nitrogen atoms are in a planar Cu_2N_2 ring around the crystallographic inversion center, with the slightly bent azide anions (N5–N6–N7, 175.8(3)°). The Cu1–N5–Cu1ⁱⁱ bridging angle (96.10(7)°) is similar to that found in complex **7** [12], while the other complexes listed in **Table 3** show somewhat narrower bridging angles ranging from 89.9(4) to 94.77(12)°. The azide anions bridge the Cu(II) centers in an end-on fashion leading to a Cu1...Cu1ⁱⁱ separation of 3.3929(4.) Å [symmetry operation used to generate equivalent atoms: $ii = 1.5-x, 1/2-y, 1-z$]. The complexes **3–7** [7,10,12–14] show slightly shorter separation of the Cu(II) ions within Cu_2N_2 rings (3.1919(2) – 3.2978(7) Å) with respect to that observed in **2**. In the analyzed complexes, the out-of plane deviation (δ) of the azide anions spans the range from 42.56(15)° (for **5** [10]) to 52.27(15)° (for **2**). Similarly, as in complex **1** the orientation of the $N(CH_3)_3$ group is supported by the intramolecular C_{Me} -

H \cdots O_{enolate} hydrogen bonds (**Table S1** in the Supporting information). The dihedral angle N4-C9-C8-N3 is 155.9(2) $^\circ$ and the distance of N4 atom from the mean coordination plane (Cu1, N1, N2, O1, N5) is 0.589(2) Å. In the environment of the Cu(II) ion a long non-bonding Cu1 \cdots O5 contact of 2.801(2) Å was observed (**Fig. 3**). Taking into account this observation, the geometry around Cu(II) ion could be described as tetragonally elongated octahedral with N_{azide}-Cu-O_{perchlorate} bond angle of 173.64(6) $^\circ$. The dinuclear units of **2** are connected by means of C_{Me}-H \cdots N_{azide} hydrogen bonds into 1D chains extending parallel with the [1 -1 0] direction (**Table S1** and **Fig. S2**).

Table 3

Structural parameters correlating the geometry of square pyramidal di(μ -_{1,1}-azido) bridged Cu(II) complexes with hydrazone-based ligands.

Complex	Cu-N _{azido(end-on)} -Cu ($^\circ$)	δ^a ($^\circ$)	Cu \cdots Cu (Å)	Cu-N _{azido(end-on)} (Å)	τ_5^b	ρ (Å) ^c	Ref.
[Cu ₂ L ₂ (N ₃) ₂](ClO ₄) ₂ (2)	96.10(7)	52.27(15)	3.3929(4)	1.9333(17) 2.590(2)	0.27	0.0064(3)	This work
[Cu ₂ (L ¹) ₂ (N ₃) ₂] ^d (3)	89.9(4)	50.2(8)	3.205(6)	1.968(9) 2.534(10)	0.27	0.045(2)	[13]
[Cu ₂ (L ²) ₂ (N ₃) ₂] ^e (4)	92.31(7)	49.97(15)	3.242(4)	1.9454(19) 2.5164(19)	0.27	0.0488(3)	[14]
[Cu ₂ (L ³) ₂ (N ₃) ₂] ^f (5)	91.53(7)	42.56(15)	3.1919(2)	1.9401(2) 2.4832(2)	0.29	0.0486(3)	[10]
[Cu ₂ (L ⁴) ₂ (N ₃) ₂] ^g (6)	94.77(12)	43.2(2)	3.272(1)	1.939(3) 2.478(3)	0.26	0.0410(4)	[7]
[Cu ₂ (L ⁵) ₂ (N ₃) ₂] ^h (7)	96.35(7)	47.16(15)	3.2978(7)	1.9640(18) 2.4409(17)	0.22	0.0887(3)	[12]

^a δ ($^\circ$) is the out-of-plane deviation of the azide ion measured as the angle between Cu₂N₂ plane and the N-N bond.

^b The parameter τ_5 ($\tau_5 = (\beta - \alpha)/60$, where β and α are the two largest angles around the central atom) is an index of the degree of trigonality, within the structural continuum between trigonal bipyramidal and square-based pyramidal geometry.

^c ρ (Å) is the distance of metal ion from the mean basal plane of square pyramid toward the apical ligand.

^d L¹ = condensation product of benzhydrazide and 2-acetylpyridine.

^e L² = 2-benzoylpyridine-3-methoxybenzhydrazone.

^f L³ = pyridine 2-carbaldehyde 4-hydroxy benzoyl hydrazone.

^g L⁴ = (*E*)-*N'*-(phenyl(pyridin-2-yl)methylene)isonicotinohydrazide.

^h L⁵ = methyl 2-pyridyl ketone semicarbazone.

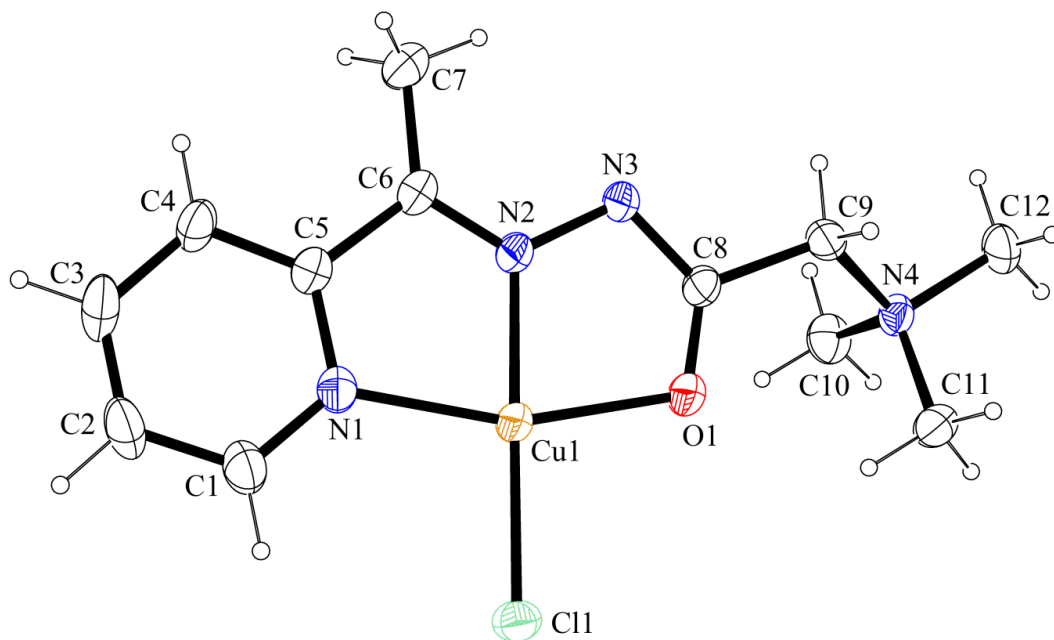


Fig. 1. ORTEP presentation [65,66] of the complex cation $[\text{CuLCl}]^+$ in $[\text{CuLCl}]\text{ClO}_4$ (**1**). Thermal ellipsoids are drawn at the 30% probability level.

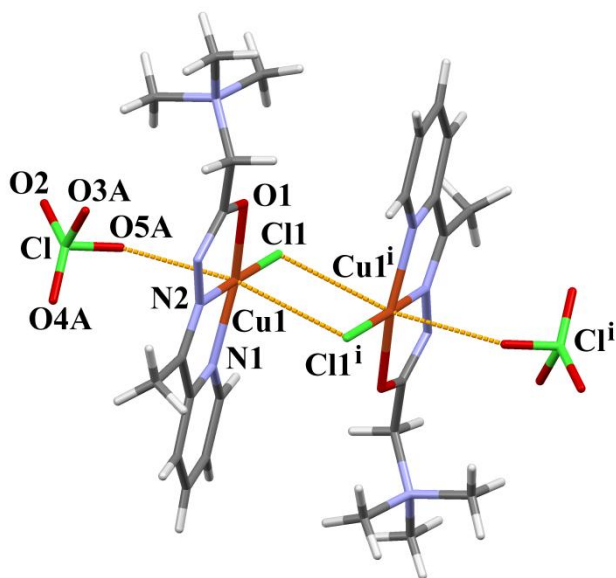


Fig. 2. View of the dimeric unit of **1** of pseudo-octahedral geometry. Long non-bonding contacts $\text{Cu}\cdots\text{O}$ and $\text{Cu}\cdots\text{Cl}$ are represented as dashed orange lines. Symmetry code *i* stands for $-x, -y, 1-z$. ClO_4^- anion suffers from the positional disorder.

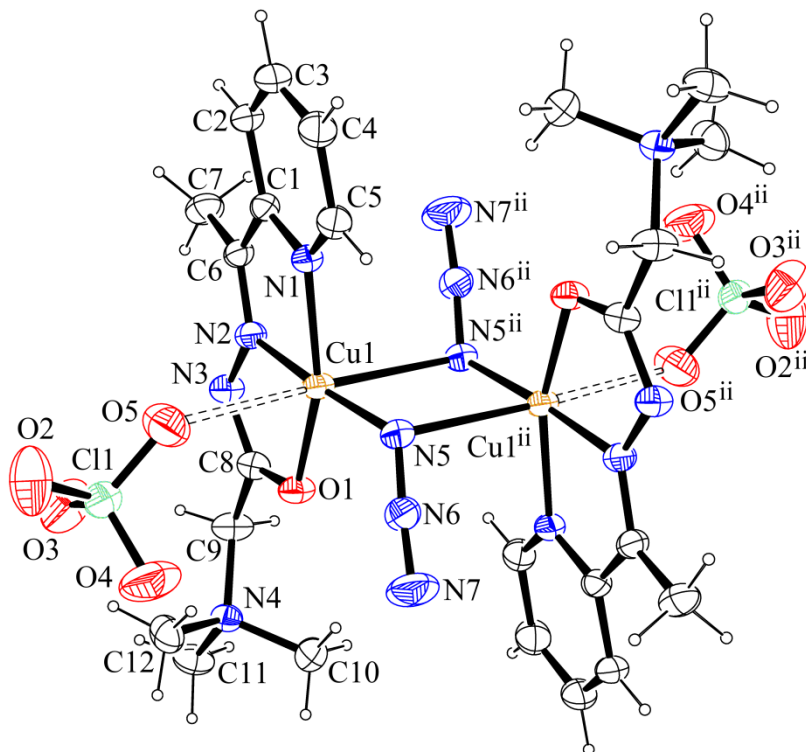


Fig. 3. ORTEP presentation of the dimeric unit of **2**. Thermal ellipsoids are drawn at the 30% probability level. Non-bonding contacts between Cu and O atoms are represented as dashed lines. Symmetry codes: ii = 1.5-x, 1/2-y, 1-z.

3.4. Magnetic measurements

A measurement of the temperature dependence of susceptibility in a static magnetic field of 1 kOe for **2** is shown in **Fig. 4** as a product of the magnetic susceptibility and temperature versus temperature. Instead of a horizontal line, which would be expected for a system of non-interacting magnetic moments (Curie law), the curve strongly rises as the temperature gets lower. In addition, the value for magnetic susceptibility measured at 300 K gives an effective magnetic moment $\mu_{eff} = 2.3 \mu_B$ per magnetic ion (as calculated from the Curie constant), which is considerably greater than expected for Cu^{2+} ion ($1.9 \mu_B$, [67]). Both observations clearly imply local ferromagnetic interactions between spins localized on an ion pair.

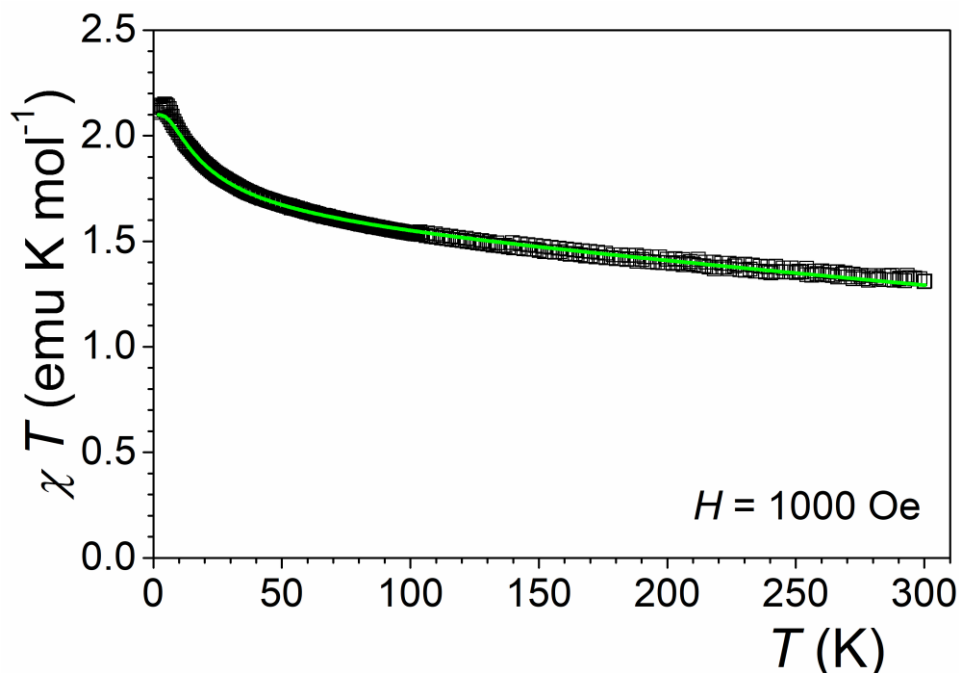


Fig. 4. Product of susceptibility χ and temperature T as a function of temperature. A full green line is a fit with function (1).

In order to estimate the magnitude of the intramolecular ferromagnetic coupling, the magnetic data (the product χ^*T) were fitted to the Bleaney-Bowers equation:

$$\chi \cdot T = \frac{2 N_A g^2 \mu_B^2}{k (3 + e^{-\frac{2J}{kT}})} \quad (1)$$

for two interacting copper(II) ions with the interaction Hamiltonian in the form $H = -2 J \mathbf{S}_1 \cdot \mathbf{S}_2$ [68]. The least-squares fitting of the data with equation 1 leads to the interaction parameter $J = +7.4 \text{ cm}^{-1}$. The theoretical curve is shown as a solid line in **Fig. 4**.

3.5. DFT calculations

To explain the origin of the ferromagnetic ground state of the dimer **2** broken-symmetry DFT calculations were performed based on the X-ray data. Calculated J in $[\text{Cu}_2\text{L}_2(\text{N}_3)_2]^{2+}$ at the BP86/def2-TZVP level of theory is $+5.36 \text{ cm}^{-1}$. This is in excellent agreement with experimentally determined $J_{\text{exp}} = +7.4 \text{ cm}^{-1}$. Taking into account perchlorate anions in

calculations, i.e. considering $[\text{Cu}_2\text{L}_2(\text{N}_3)_2](\text{ClO}_4)_2$ complex, gives even better agreement with experiment, calculated $J = +7.73 \text{ cm}^{-1}$. Weak ferromagnetic coupling is observed irrespectively of the level of theory employed (see Supplementary material). As explained in the discussion of the crystal structure of **2**, the geometry around Cu(II) ions can be considered either as elongated square pyramidal or elongated octahedral. In both cases, the unpaired electron is in the local $d_{x^2-y^2}$ orbital, while the local d_z^2 contains spin paired electrons. The spin density in the ground ferromagnetic state is mainly located in the equatorial plane of the subunits, **Fig. 5**. There is an extensive delocalization of the spin density towards directly coordinated equatorial donor atoms (N1, N2, O1, N5) and toward terminal nitrogen atom of the azide group (N7), **Fig. 5** and **Table 4**. All the atoms with considerable spin density have the same sign. The middle nitrogen atoms of the bridging azide ligands (N6) have a very small negative spin population. This distribution of the spin density indicates that spin delocalization is the main exchange mechanism. Weak coupling is due to the nature of the bridge between monomeric units. Azido bridge is linked in equatorial fashion to one Cu(II), but in axial to the second. Spin density is delocalized from one Cu(II) to the bridging nitrogen atom (N5), but delocalization from the second Cu(II) is poor because bridging nitrogen is in axial position with a longer Cu1ⁱⁱ-N5 distance. The situation is equivalent for the second azide group. Consequently, the weak coupling is expected, as observed. Weak ferromagnetic coupling can be understood based on the analysis of the unrestricted corresponding orbitals [56] obtained from the broken-symmetry determinant, **Fig. 6**. Magnetic orbital centered on the one Cu(II) is parallelly displaced to the orbital centered on the other Cu(II). The equatorial-axial coordination of the bridging azide, and long axial Cu-N5 distance causes poor orbital overlap. Calculated overlap is 0.016 at the BP86/def2-TZVP level of theory for $[\text{Cu}_2\text{L}_2(\text{N}_3)_2](\text{ClO}_4)_2$. Such a small overlap implies that the antiferromagnetic coupling is quenched completely [69]. Thus, the ferromagnetic exchange interaction in **2** is favored.

Table 4

Mulliken spin densities for dimer **2** calculated at the BP86/ZORA-def2-TZVP level of theory.

	$[\text{Cu}_2\text{L}_2(\text{N}_3)_2]^{2+}$	$[\text{Cu}_2\text{L}_2(\text{N}_3)_2](\text{ClO}_4)_2$
Cu1	0.489	0.509
N1	0.099	0.087
N2	0.128	0.119

O1	0.082	0.074
N5	0.083	0.086
N6	-0.021	-0.022
N7	0.104	0.111

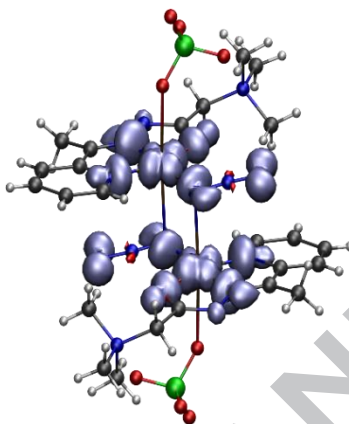


Fig. 5. Graphical representation of the spin density of the high-spin state of the dimer (**2**). Isosurfaces were drawn at $0.003 \text{ e}/\text{\AA}^3$ with α -spin depicted by blue surfaces and β -spin depicted by red surfaces.

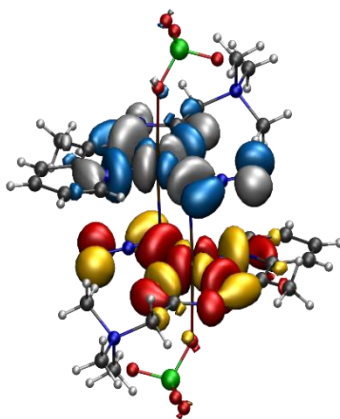


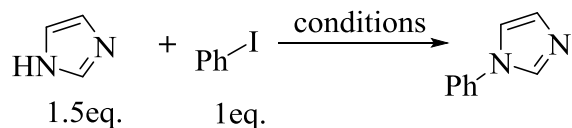
Fig. 6. Unrestricted corresponding orbitals obtained from the broken-symmetry solution of the dimer **2**. α Spin-orbitals are depicted as red (positive)/yellow (negative) lobes; β spin-orbitals are

depicted as blue (positive)/grey (negative) lobes. Isosurfaces were drawn at $0.03 \text{ e}/\text{\AA}^3$. Their spatial overlap is 0.016.

3.6. Catalysis

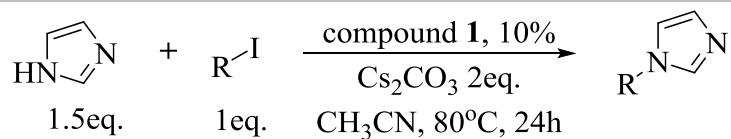
The reaction between iodobenzene and imidazole [70,71] was chosen as the benchmark reaction for our optimization studies. As shown in **Table 5**, CuI and CuBr₂ exhibit low reactivity, towards the formation of the desired product, when Cs₂CO₃ was used as base in acetonitrile at 80°C. CuCl₂ and CuCl provided better yields, affording 1-phenylimidazole in 24 and 37% yield, respectively (entries 3 and 4, **Table 5**). On the other hand, **1** provided excellent isolated yields, affording 1-phenylimidazole almost quantitatively under identical conditions (10% loading). At 8% catalyst loading (entry 7, **Table 5**) the yield of the reaction decreased to 84%.. A number of other bases and solvents were also tested during the optimization of the reaction conditions (**Table 5**). Triethylamine [72] was found to be incompatible with the reaction, while NaOH afforded an 89% yield under the same conditions. Besides acetonitrile, DMF and THF were also tested as solvents. In both cases, the reaction afforded the desired product, albeit in lower yield than acetonitrile. Based on the optimization studies, the reaction affords excellent yields under 10% catalyst loading in the presence of two equivalents of cesium carbonate, in acetonitrile when conducted at 80°C for 24h (entry 1 **Table 6**, and entry 1 **Table 7**).

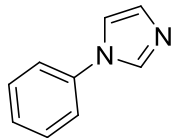
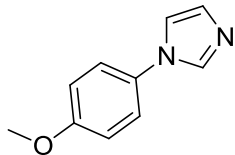
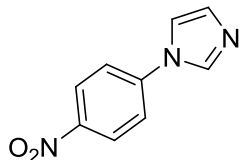
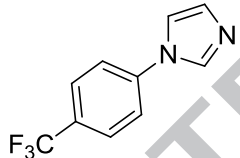

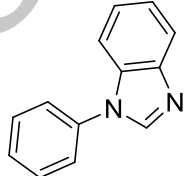
With the optimized reaction conditions in hand, we explored the reactivity of both **1** and **2**. A number of *N*-substituted imidazoles and benzimidazoles were successfully synthesized. As shown in **Tables 6** and **7**, both catalysts show excellent reactivity in affording *N*-arylated imidazoles with aryl groups bearing either electron-donating or electron-withdrawing moieties. In addition, both catalysts exhibit similar reaction profiles when the scope of the reaction is expanded to benzimidazole derivatives (entries 6, 7 **Table 6**, and 2, 7 **Table 7**). *Para*-iodophenol was also utilized, but did not provide the desired product (entry 8, **Table 6**). On the other hand, *p*-iodoaniline and *m*-iodopyridine provided the corresponding derivatives in very good yields (entries 9-10, **Table 6**). Overall, both **1** and **2** are excellent catalysts in the synthesis of *N*-arylatedimidazoles and benzimidazoles.

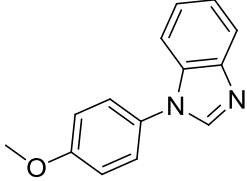
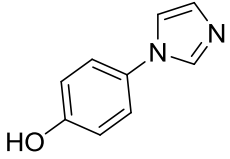
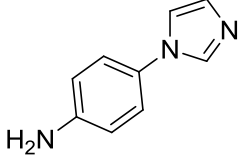
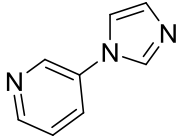
Table 5*N*-arylation of imidazole – optimization conditions.

Entry	Catalyst	Catalyst loading	Base	Solvent	Reaction yield (%)
1	-	-	Cs ₂ CO ₃	CH ₃ CN	-
2	CuBr ₂	10%	Cs ₂ CO ₃	CH ₃ CN	11
3	CuCl ₂	10%	Cs ₂ CO ₃	CH ₃ CN	24
4	CuCl	10%	Cs ₂ CO ₃	CH ₃ CN	37
5	CuI	10%	Cs ₂ CO ₃	CH ₃ CN	12
6	Compound 1	10%	Cs ₂ CO ₃	CH ₃ CN	>99
7	Compound 1	8%	Cs ₂ CO ₃	CH ₃ CN	84
8	Compound 1	10%	NaOH	CH ₃ CN	89
9	Compound 1	10%	Et ₃ N	CH ₃ CN	0
10	Compound 1	10%	K ₂ CO ₃	CH ₃ CN	47
11	Compound 1	10%	Cs ₂ CO ₃	DMF	91
12	Compound 1	10%	Cs ₂ CO ₃	THF	89

Table 6*N*-arylatedimidazoles obtained under **1** catalysis.



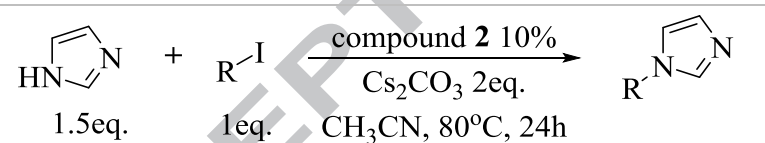
Entry	Product	Isolated yield (%)
1		99%
2		99%
3		98%
4		99%
5		99%
6		99%

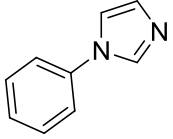
7		99%
8		No Reaction
9		78%
10		88%

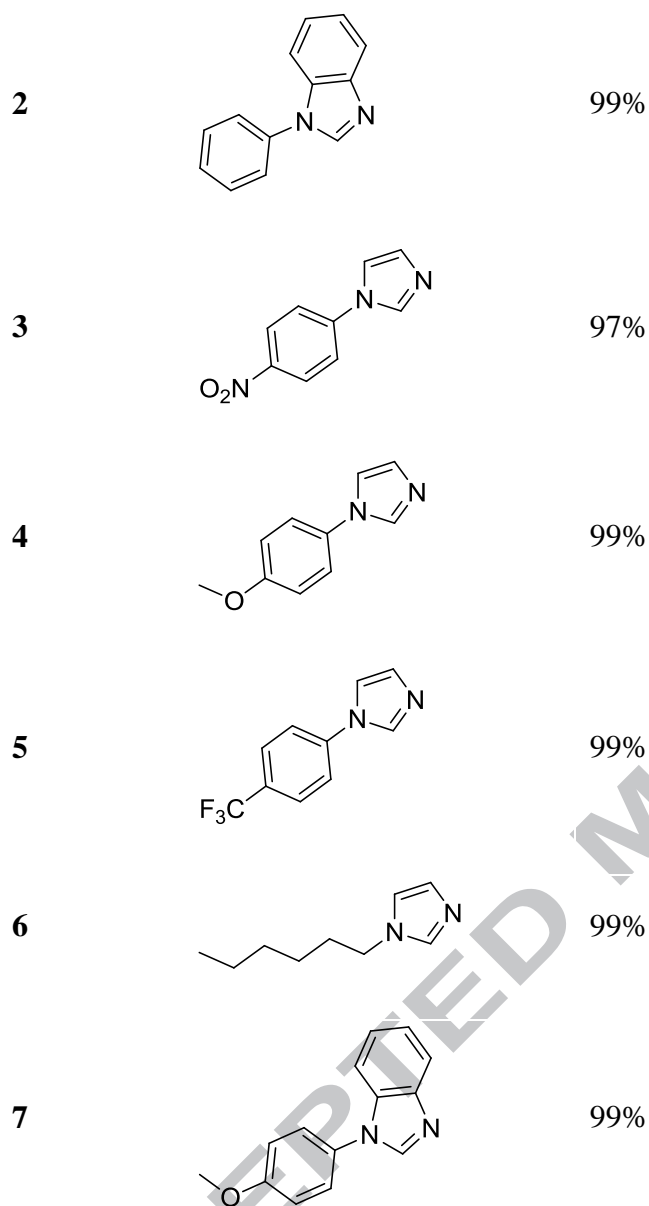
Reaction conditions: aryl halide (0.5 mmol), imidazole (0.75 mmol), Cs₂CO₃ (1.0 mmol), complex **1** (0.05 mmol), CH₃CN (0.3 mL), 80 °C, t=24h.

Table 7

N-arylated imidazoles obtained under **2** catalysis.



Entry	Product	Isolated yield (%)
1		99%



Reaction conditions: aryl halide (0.5 mmol), imidazole (0.75 mmol), Cs_2CO_3 (1.0 mmol), complex **2** (0.05 mmol), CH_3CN (0.3 mL), 80 °C, t=24h.

Although we did not study the mechanism of this transformation, two catalytic cycles proposed in the literature account for the copper-catalyzed arylation of nucleophiles such as imidazoles. According to the first proposed cycle, coordination of the nucleophile (imidazole) takes place before the oxidative addition of the aryl halide, which is then followed by the formation of the coupling product via reductive elimination. According to the second scenario,

oxidative addition of the aryl halide occurs in the first step, prior to the coordination of the nucleophile [32,73].

4. Conclusion

In this paper, we presented a comprehensive discussion on the synthesis and structural characterizations of mononuclear and dinuclear azido double end-on bridged Cu(II) complexes with condensation product of 2-acetylpyridine and Girard's T reagent. Variable- temperature magnetic susceptibility studies for dinuclear Cu(II) complex showed intramolecular ferromagnetic coupling between Cu(II) ions with interaction parameter $J = + 7.4 \text{ cm}^{-1}$. Broken-symmetry DFT calculations based on the X-ray crystal structure of $[\text{Cu}_2\text{L}_2(\text{N}_3)_2](\text{ClO}_4)_2$ complex were performed to explain the origin of the ferromagnetic ground state. Calculated J in $[\text{Cu}_2\text{L}_2(\text{N}_3)_2]^{2+}$ at the BP86/def2-TZVP level of theory is $+5.36 \text{ cm}^{-1}$. Taking into account perchlorate anions in calculations obtained value for J is $+7.73 \text{ cm}^{-1}$. This is in excellent agreement with experimentally determined $J_{\text{exp}} = +7.4 \text{ cm}^{-1}$. Weak ferromagnetic coupling is observed irrespectively of the level of theory employed. The investigated complexes catalyze the *N*-arylation of imidazole and benzimidazole with alkyl iodides, as well as electron-poor or electron-rich aryl iodides, in a highly-efficient, user-friendly and sustainable protocol.

Acknowledgements

This work was supported by the Ministry of Education, Science and Technological development of the Republic of Serbia (Grant OI 172055) and the Slovenian Research Agency (P-0175 and P2-0348) which enabled the postdoctoral stay of Božidar Čobeljić at the University of Ljubljana (labs of I. Turel). We thank the EN-FIST Centre of Excellence, Ljubljana, Slovenia, for use of the SuperNova diffractometer. We also acknowledge the contribution of COST Action CA15106 (C-H Activation in Organic Synthesis – CHAOS), as well as the Special Account for Research Grants of the National and Kapodistrian University of Athens (Research Program 70/3/14872).

References

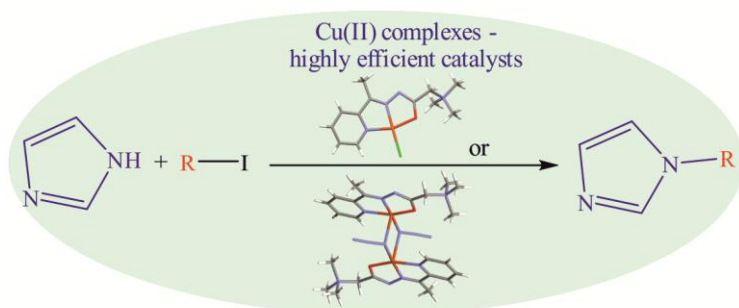
- [1] C. Aronica, E. Jeanneau, H.E. Moll, D. Luneau, B. Gillon, A. Goujon, A. Cousson, M.A. Carvajal, V. Robert, *Chem. Eur. J.* 13 (2007) 3666–3674.
- [2] S. Triki, C.J. Gomez-Garcia, E. Ruiz, J. Sala-Pala, *Inorg. Chem.* 44 (2005) 5501–5508.
- [3] F.R. Louka, S.S. Massoud, T.K. Haq, M. Koikawa, M. Mikuriya, M. Omote, R.C. Fischer, F.A. Mautner, *Polyhedron* 138 (2017) 177–184.
- [4] A. Bhattacharyya, A. Bauzá, S. Sproules, L.S. Natrajan, A. Frontera, S. Chattopadhyay, *Polyhedron* 137 (2017) 332–346.
- [5] I.V. Pankov, I.N. Shcherbakov, V.V. Tkachev, S.I. Levchenkov, L.D. Popov, V.V. Lukov, S.M. Aldoshin, V.A. Kogan, *Polyhedron* 135 (2017) 237–246.
- [6] S. Saha, D. Biswas, P.P. Chakrabarty, A.D. Jana, A.K. Boudalis, S.K. Seth, T. Kar, *Polyhedron* 29 (2010) 3342–3348.
- [7] H. Hosseini-Monfared, R. Bikas, R. Szymczak, P. Aleshkevych, A.M. Owczarzak, M. Kubicki, *Polyhedron* 63 (2013) 74–82.
- [8] P.P. Chakrabarty, S. Giri, D. Schollmeyer, H. Sakiyama, M. Mikuriya, A. Sarkar, S. Saha, *Polyhedron* 89 (2015) 49–54.
- [9] P. Bhowmik, A. Bhattacharyya, K. Harms, S. Sproules, S. Chattopadhyay, *Polyhedron* 85 (2015) 221–231.
- [10] B. Shaabani, A.A. Khandar, H. Mobaiyen, N. Ramazani, S.S. Balula, L. Cunha-Silva, *Polyhedron* 80 (2014) 166–172.
- [11] M. Das, B.N. Ghosh, K. Rissanen, S. Chattopadhyay, *Polyhedron* 77 (2014) 103–114.
- [12] B. Shaabani, A.A. Khandar, F. Mahmoudi, M.A. Maestro, S.S. Balula, L. Cunha-Silva, *Polyhedron* 57 (2013) 118–126.
- [13] S. Sen, S. Mitra, D.L. Hughes, G. Rosair, C. Desplanches, *Polyhedron* 26 (2007) 1740–1744.
- [14] M.M. Fousiamol, M. Sithambaresan, V.A. Smolenski, J.P. Jasinski, M.R.P. Kurup, *Polyhedron* 141 (2018) 60–68.
- [15] M.R. Milenković, B. Čobeljić, K. Anđelković, I. Turel, *Eur. J. Inorg. Chem.* (2018) 838–846.

- [16] B. Forte, B. Malgesini, C. Piutti, F. Quartieri, A. Scolaro, G. Papeo, *Mar. Drugs* 7 (2009) 705–753.
- [17] Z. Jin, *Nat. Prod. Rep.* 28 (2011) 1143–1191.
- [18] H. Jiang, C. Zhou, K. Luo, H. Chen, J. Lan, R. Xie, *J. Mol. Catal. A-Chem.* 260 (2006) 288–294.
- [19] G. Gao, R. Xiao, Y. Yuan, C. Zhou, J. You, R. Xie, *J. Chem. Res.* 2002 (2002) 262–263.
- [20] L. Zhang, X. Peng, G. Damu, R. Geng, C. Zhou, *Med. Res. Rev.* 34 (2013) 340–437.
- [21] F. Xue, C. Cai, H. Sun, Q. Shen, J. Rui, *Tetrahedron Lett.* 49 (2008) 4386–4389.
- [22] M. Voets, I. Antes, C. Scherer, U. Müller-Vieira, K. Biemel, C. Barassin, S. Marchais-Oberwinkler, R. Hartmann, *J. Med. Chem.* 48 (2005) 6632–6642.
- [23] N. Xi, Q. Huang, L. Liu, in: A.R. Katritzky, C.A. Ramsden, E.F.V. Scriven, R.J.K. Taylor (Eds.), *Comprehensive Heterocyclic Chemistry*, Elsevier, Oxford, 2008, vol. 4, pp. 143–364.
- [24] Z. Wang, W. Bao, Y. L. Jiang, *Chem. Commun.* 0 (2005) 2849–2851.
- [25] M. Taillefer, N. Xia, A. Ouali, *Angew. Chem. Int. Ed.* 46 (2007) 934–936.
- [26] S. Ley, A. Thomas, *Angew. Chem. Int. Ed.* 42 (2003) 5400–5449.
- [27] M. Yang, F. Liu, *J. Org. Chem.* 72 (2007) 8969–8971.
- [28] X. Lv, W. Bao, *J. Org. Chem.* 72 (2007) 3863–3867.
- [29] W. Long, W. Qiu, C. Guo, C. Li, L. Song, G. Bai, G. Zhang, H. He, *Molecules* 20 (2015) 21178–21192.
- [30] X. Zhu, L. Su, L. Huang, G. Chen, J. Wang, H. Song, Y. Wan, *Eur. J. Org. Chem.* 2009 (2009) 635–642.
- [31] Y. Wang, Z. Wu, L. Wang, Z. Li, X. Zhou, *Chem. Eur. J.* 15 (2009) 8971–8974.
- [32] H. Cristau, P. Cellier, J. Spindler, M. Taillefer, *Chem. Eur. J.* 10 (2004) 5607–5622.
- [33] Y. Wang, J. Gao, M. Zhao, J. Li, *Chem. Res. Chin. Univ.* 31 (2015) 549–552.
- [34] Y. Liu, W. Liu, Q. Zhang, P. Liu, J. Xie, B. Dai, *J. Chem. Res.* 37 (2013) 636–637.
- [35] M. Kantam, T. Ramani, L. Chakrapani, *Synthetic Commun.* 38 (2008) 626–636.
- [36] Z. Otwinowsky, W. Minor, *Methods Enzymol.* 276 (1997) 307–325.
- [37] Oxford Diffraction, *CrysAlis PRO*, Oxford Diffraction Ltd., Yarnton, England, 2009.
- [38] A. Altomare, G. Cascarano, C. Giacovazzo, A. Guagliardi, *J. Appl. Crystallogr.* 26 (1993) 343–350.

- [39] G. M. Sheldrick, *Acta Crystallogr. C* 71 (2015) 3–8.
- [40] G. Jonkers, C.A. de Lange, L. Noodleman, E.J. Baerends, *Mol. Phys.* 46 (1982) 609–620.
- [41] L. Noodleman, *J. Chem. Phys.* 74 (1981) 5737–5743.
- [42] L. Noodleman, E. R. Davidson, *Chem. Phys.* 109 (1986) 131–143.
- [43] L. Noodleman, J.G. Norman, J.H. Osborne, A. Aizman, D.A. Case, *J. Am. Chem. Soc.* 107 (1985) 3418–3426.
- [44] F. Neese, *Coord. Chem. Rev.* 253 (2009) 526–563.
- [45] T. Soda, Y. Kitagawa, T. Onishi, Y. Takano, Y. Shigeta, H. Nagao, Y. Yoshioka, K. Yamaguchi, *Chem. Phys. Lett.* 319 (2000) 223–230.
- [46] F. Neese, *Wiley Interdiscip. Rev. Comput. Mol. Sci.* 2 (2012) 73–78.
- [47] C. Wüllen, *J. Chem. Phys.* 109 (1998) 392–399.
- [48] A.D. Becke, *Phys. Rev. A* 38 (1988) 3098–3100.
- [49] J. Perdew, *Phys. Rev. B* 33 (1986) 8822–8824.
- [50] J.P. Perdew, *Phys. Rev. B* 34 (1986) 7406–7406.
- [51] F. Weigend, R. Ahlrichs, *Phys. Chem. Chem. Phys.* 7 (2005) 3297–3305.
- [52] D.A. Pantazis, X.Y. Chen, C.R. Landis, F. Neese, *J. Chem. Theory Comput.* 4 (2008) 908–919.
- [53] F. Neese, *J. Chem. Phys.* 115 (2001) 11080–11096.
- [54] D.A. Pantazis, F. Neese, *J. Chem. Theory Comput.* 5 (2009) 2229–2238.
- [55] F. Weigend, *Phys. Chem. Chem. Phys.* 8 (2006) 1057–1065.
- [56] F. Neese, *J. Phys. Chem. Solids* 65 (2004) 781–785.
- [57] Z. Liu, J. Vors, E. Gesing, C. Bolm, *Green Chem.* 13 (2011) 42–45.
- [58] L. Zhu, G. Li, L. Luo, P. Guo, J. Lan, J. You, *J. Org. Chem.* 74 (2009) 2200–2202.
- [59] P. Liu, P. Li, L. Wang, *Synth. Commun.* 42 (2012) 2595–2605.
- [60] M. Smiglak, C. Hines, W. Reichert, A. Vincek, A. Katritzky, J. Thrasher, L. Sun, P. McCrary, P. Beasley, S. Kelley, R. Rogers, *New J. Chem.* 36 (2012) 702–722.
- [61] N. Panda, A. Jena, S. Mohapatra, S. Rout, *Tetrahedron Lett.* 52 (2011) 1924–1927.
- [62] K. Nakamoto, *Infrared and Raman Spectra of Inorganic and Coordination Compounds*, fourth ed., Wiley-Interscience, New York, 1986.
- [63] L. Yang, D.R. Powell, R.P. Houser, *Dalton Trans.* (2007) 955–964.

- [64] A.W. Addison, T.N. Rao, J. Reedijk, J. Van Rijn, G.C. Verschoor, *J. Chem. Soc., Dalton Trans.* (1984) 1349–1356.
- [65] L.J. Farrugia, *J. Appl. Crystallogr.* 45 (2012) 849–854.
- [66] C.F. Macrae, P.R. Edgington, P. McCabe, E. Pidcock, G.P. Shields, R. Taylor, M. Towler, J. van de Streek, *J. Appl. Crystallogr.* 39 (2006) 453–457.
- [67] N.W. Ashcroft, N.D. Mermin, *Solid State Physics*, Saunders College Publishing, USA, 1976.
- [68] O. Kahn, *Molecular Magnetism*, VCH, New York, 1993.
- [69] D.A. Pantazis, V. Krewald, M. Orio, F. Neese, *Dalton Trans.* 39 (2010) 4959–4967.
- [70] *Chemistry of Heterocyclic Compounds: A Series Of Monographs* (2008) 3–31.
- [71] M. Lõkov, S. Tshepelevitsh, A. Heering, P. Plieger, R. Vianello, I. Leito, *Eur. J. Org. Chem.* 2017 (2017) 4475–4489.
- [72] J. Ammer, M. Baidya, S. Kobayashi, H. Mayr, *J. Phys. Org. Chem.* 23 (2010) 1029–1035.
- [73] F. Monnier, M. Taillefer, *Angew. Chem., Int. Ed.* 48 (2009) 6954–6971.

Graphical abstract



The cover picture shows crystal structures of mono- and dinuclear Cu(II) complexes with the condensation product of 2-acetylpyridine and Girard's T reagent. Catalytic properties of Cu(II) complexes in *N*-arylation of imidazole and benzimidazole with alkyl and aryl iodides were investigated.